I&EC research
Industrial & Engineering Chemistry Research

pubs.acs.org/IECR

Article

One-Pot Synthesis of Menthol Starting from Citral over Ni Supported on Attapulgite-H-Beta-38 Extrudates in a Continuous Flow: Effect of Metal Location

Irina L. Simakova, Päivi Mäki-Arvela, Mark Martínez-Klimov, Joseph Muller, Zuzana Vajglová, Markus Peurla, Kari Eränen, and Dmitry Yu. Murzin*

Cite This: *Ind. Eng. Chem. Res.* 2022, 61, 12998−13010

Read Online

ACCESS | Metrics & More | Article Recommendations | Supporting Information

ABSTRACT: The one-pot synthesis of menthol from citral in a continuous mode was investigated over three different types of extrudates, namely Ni supported on H-Beta-38 and extruded with attapulgite, Ni supported on attapulgite and extruded with H-Beta-38, and the extrudates, which were shaped after deposition of Ni on both H-Beta-38 and attapulgite in the powder form. These composite catalysts were characterized by X-ray diffraction, transmission and scanning electron microscopy, temperature-programmed reduction of H_2, mechanical strength, and pyridine adsorption desorption. These three types of extrudates exhibited different metal particle sizes and acidity. The most promising catalyst in the one-pot menthol synthesis was Ni supported first on H-Beta-38 and then extruded with attapulgite giving a 45% yield of menthols in a trickle bed reactor. This catalyst exhibited 10 nm nickel particles and a rather high amount of strong Brønsted acid sites.

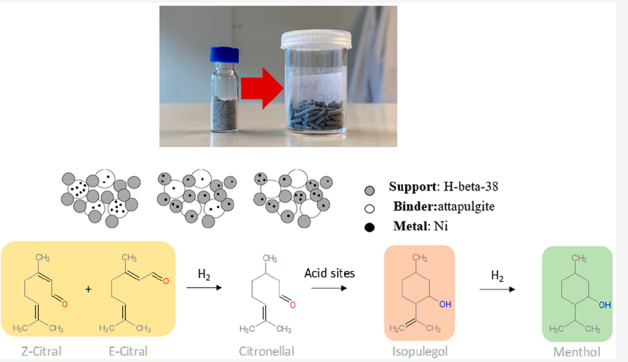

1. INTRODUCTION

Menthol is an important product used in pharmaceuticals including mouthwash, toothpaste, chewing gum, tobacco, candy, and cosmetics.[1] It is obtained from peppermint and cornmint oil, and it is also produced synthetically starting from thymol or myrcene.[2] The one-pot synthesis of menthol from citronellal has been intensively investigated using both supported noble[3−9] and transition metal catalysts.[10−13] The highest yields of menthols in a batch reactor have been obtained over Ni/Zr-Beta catalysts giving the menthol yield of 86−97%.[11] In ref 11, citronellal transformations to isopulegol were performed first under helium atmosphere, followed by hydrogenation. An analogous strategy was used in ref 13 reporting 86% yield of menthol under 1 bar hydrogen at 90 °C starting from citronellal. Menthol synthesis from citral (Figure 1), which is also a naturally occurring compound, obtained especially from lemongrass oil, has been scarcely studied.[2,14−19] Mainly such a one-pot synthesis of menthol from citral has been investigated in batch reactors with the best results reported for Ni-supported catalysts.[2] The highest menthol yield, 94%, was obtained in a batch reactor over 8 wt % Ni/Al-MCM-41 at 70 °C and 20.2 bar hydrogen.[14] In the previous work of the authors, it was demonstrated that Ru containing catalysts in the form of extrudates can be used in the one-pot synthesis of menthol in a trickle bed reactor.[17,18] These catalysts were not, however, selective toward menthol formation. For example, Ru-MCM-41 and Ru-H-Y-80 gave maximally 6% menthol yields, while defunctionalized menthane derivatives were the major products.[17,18]

Encouraged by the promising results in a batch reactor with supported bifunctional nickel catalysts,[2,14] the aim in this work was to demonstrate menthol production in a trickle bed reactor over Ni extrudates. The authors have recently demonstrated the suitability of Ni-H-Beta-38 sepiolite extrudates (the number denotes the Si/Al ratio) as catalysts in the one-pot synthesis of menthol starting from citronellal and citral.[20] This Ni-H-Beta-38-sepiolite catalyst prepared by impregnation of extrudates and subsequently having Ni located both on H-Beta-zeolite and sepiolite gave a 49% yield of menthols and 72−74% stereoselectivity. Furthermore, continuous transformation of citral over Ni supported on a mesoporous aluminosilicate using sepiolite as a binder at 70 °C was reported giving 75% selectivity to menthols.[21]

In the current work, Ni containing extrudates composed of H-Beta-38 zeolite and attapulgite clay as a binder alternative to sepiolite[20] were prepared, characterized, and tested in one-pot

Received: June 30, 2022
Revised: August 14, 2022
Accepted: August 14, 2022
Published: August 25, 2022

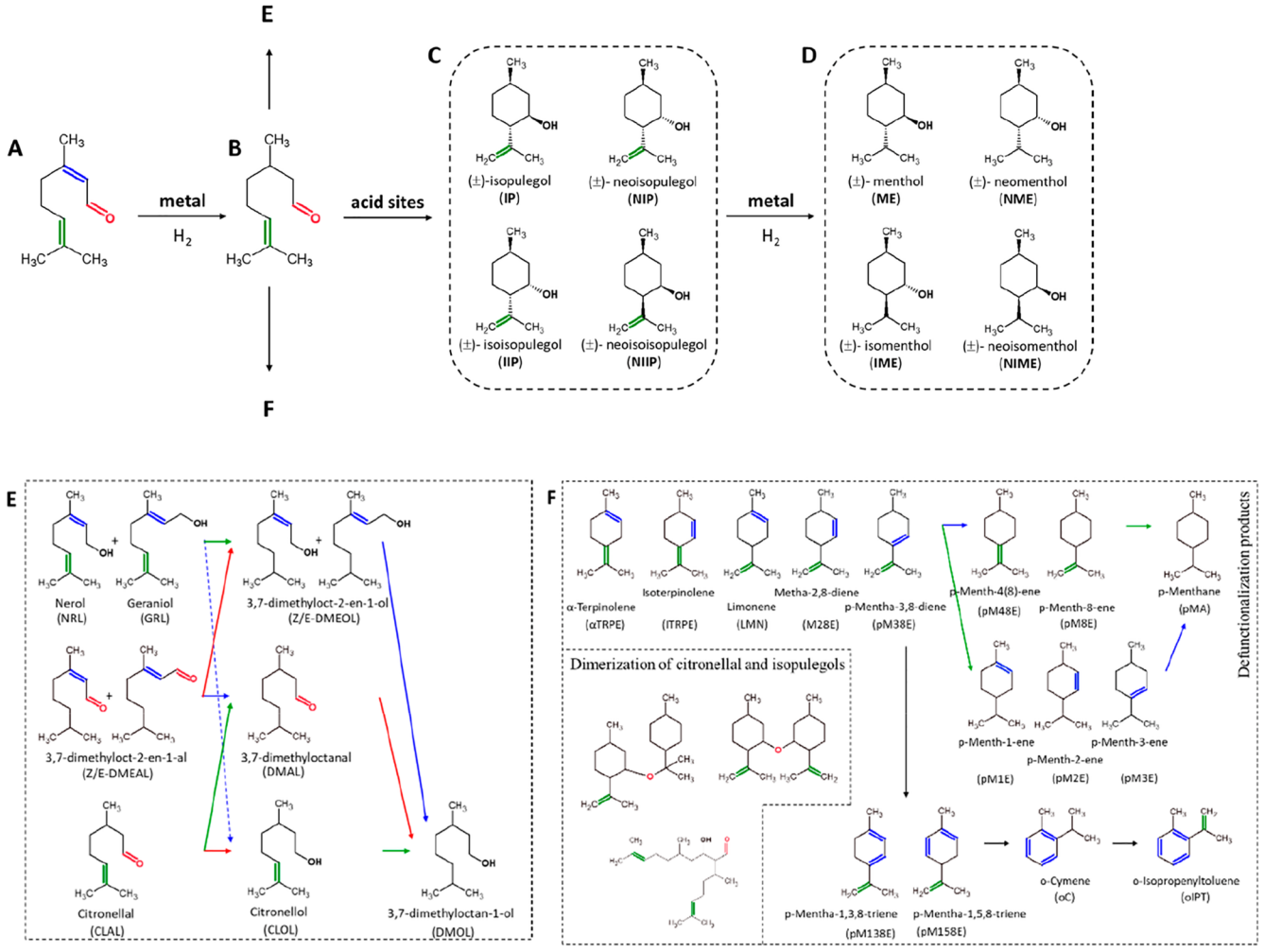

Figure 1. Reaction scheme for citral transformation to menthol. Legend: A − citral, B − citronellal, C − isopulegol isomers, D − menthol isomers, E − acyclic hydrogenation products, F − defunctionalization products, dimeric ethers, and heavy components.

transformation of citral to menthol in a trickle bed reactor. A bifunctional catalyst with suitable acidity and a metal particle size is required for selective synthesis of menthol from citral as follows from data generated in a batch reactor.[14] Beta zeolite with the Si/Al ratio of 25 has been a promising support for Ni in citral transformations to menthol in that study;[14] thus, a commercially available acidic H-Beta-38 was selected as a support together with attapulgite as a binder for citral transformation to menthols. Attapulgite, a naturally occurring magnesium aluminum silicate clay mineral with the chemical formula $[(Mg,Al)_4Si_8(O, OH, H_2O)_{24}{\cdot}nH_2O]$,[22] exhibits a chain layered crystal structure and a large specific surface area.[23] Attapulgite being typically mildly acidic is often applied as a binder for extrusion and has been also successfully used as a support per se for nickel in the hydrogenation of maleic anhydride[24] and vegetable oil.[25]

Although clays have been used as binders in extrudates with the main purpose to ensure the mechanical strength and stability of the extrudates, different binders exhibit different Si/Al ratios, hydrophobicity, and textural properties, being not necessarily inert in terms of their catalytic behavior.[29] Furthermore, it was shown in ref 29 that different optimum amounts of water are required to make extrudates from various clays. Taking into account all these parameters, it cannot be predicted beforehand how exactly a composite material comprising Ni supported on attapulgite-H-Beta-38 will work in a complex reaction, citral transformation to menthol.

The aim of this work was to prepare composite catalysts in the extrudate form using three different methods: loading on extrudates prepared from a mixture of H-Beta-38 and attapulgite or alternatively depositing Ni either on attapulgite and extruded with H-Beta-38 or loading of Ni on H-Beta-38 and extruding it with attapulgite. The importance of metal location in extrudates has been earlier emphasized especially in citral transformation to menthol,[20] and the hydroisomerization reaction in refs 26−28 and the close proximity of a metal and an acid site have been found to be of crucial importance in selective hydroisomerization. Furthermore, it was recently observed in citral transformations to menthols that even with the same catalyst in the powder and in extrudate forms different product distributions were obtained in batch and continuous reactors.[18] There is apparently a lack of experimental data for other reactions of a similar type involving the central metal and acid, such as the one-pot synthesis of menthol in a continuous reactor with extruded catalysts, and it is difficult to predict the product distribution in advance for the bifunctional extrudates, because several physicochemical processes occur during production of extrudates including the mechanical impact already during preparation of a suspension for extrusion.

https://doi.org/10.1021/acs.iecr.2c02345
Ind. Eng. Chem. Res. 2022, 61, 12998−13010

Ni-H-Beta-38-sepiolite composite catalysts have been already tested in citral transformation to menthols.[20] In the current work, Ni-H-Beta-38-attapulgite composite catalysts were investigated in the same reaction under comparative conditions in a trickle bed reactor. The main differences in attapulgite and sepiolite are the higher amount of magnesium and traces of K in the latter one, while on the other hand, attapulgite contained various impurities, such as K, Fe, P, and Ca. Both clays exhibited a fibrous structure; however, the fibers in sepiolite were slightly longer and thicker in comparison to attapulgite fibers.[29] The Ni-H-Beta-H-attapulgite composite catalysts in the current work were characterized by determining their structure, acidity, and specific surface area of the metal particle size distribution to find a correlation between the catalyst properties and their performance in the one-pot synthesis of menthol. Furthermore, mechanical strength of the prepared extrudates containing attapulgite as a binder was also determined showing promising results.

2. EXPERIMENTAL SECTION

2.1. Synthesis of Catalysts. Three different modes of Ni introduction by the incipient wetness impregnation were implemented: deposition on H-Beta-38 followed by extrusion with attapulgite, introduction of attapulgite followed by extrusion with H-Beta-38, or nickel deposition on the extrudates prepared from a suspension of H-Beta-38 and attapulgite. For preparation of Ni-bearing extrudates where Ni is deposited on both H-Beta-38 and attapulgite, the commercial H-Beta-38 (SiO_2/Al_2O_3 = 38) zeolite (Zeolyst International) as an active phase and attapulgite as a binder were ground, dried overnight at 100 °C, and mixed in the mass ratio = 70/30, e.g., 4.2 and 1.8 g, respectively. Methylcellulose (1.0 wt %, e.g., 0.06 g) as an organic binder (viscosity: 4000 cP, Sigma-Aldrich) was dissolved in 3 mL of water and added into the mixture to control the rheological properties of the final slurry. Distilled water was added gradually into the suspension under constant stirring at room temperature until a soft elastic paste was prepared. The extrudates were fabricated in a cylindrical shape with a diameter of 1.4 mm using the extruder (TBL-2, Tianjin Tianda Beiyang Chemical Co. Ltd., China) at an ca. 12 cm/min extrusion rate driven by the rotational velocity of 1400 rpm. Subsequently, the extrudates were dried in an oven at 100 °C overnight, calcined at 500 °C for 4 h in a muffle oven, and cut to a length of ca. 0.6−1.0 cm. The obtained extrudates were impregnated by a nickel nitrate $Ni(NO_3)_2{\cdot}6H_2O$ (CJSC Souzchimprom) aqueous solution to achieve the nominal nickel loading 5 wt %. Thereafter, Ni-bearing extrudates were dried overnight at 100 °C followed by calcination at 450 °C for 6 h in a muffle oven.

For the preparation of Ni-containing extrudates where Ni was deposited on H-Beta-38 or on attapulgite, the ground and dried zeolite or the binder, respectively, in the powder form was impregnated with the nickel nitrate $Ni(NO_3)_2{\cdot}6H_2O$ aqueous solution to achieve the nominal metal loading 5 wt % Ni in the final catalyst. Thereafter, the suspension was dried at 100 °C overnight and calcined at 450 °C for 6 h in a muffle oven to decompose nickel nitrate. Then, the calculated amounts of attapulgite or H-Beta-38, respectively, as well as methylcellulose (1.0 wt %, 0.06 g) dissolved in 3 mL of water were mixed with a Ni-containing powder at a room temperature. Distilled water was added gradually under constant stirring at room temperature until a soft elastic paste was prepared for extrudate fabrication according to the above-mentioned procedure. The extrudates were dried overnight at 100 °C and then calcined at 500 °C for 4 h in a muffle oven.

Before each catalytic experiment, all Ni catalysts were reduced in situ in a 100 mL/min hydrogen flow at 350 °C during 2.5 h with the 2 °C/min temperature ramp.

2.2. Characterization of Catalysts. Textural properties of the catalysts were determined using nitrogen physisorption (Micrometrics 3Flex-3500). The specific surface area and pore volumes were determined using Dubinin−Radushkevich or Brunauer−Emmett−Teller (BET) and density functional theory (DFT) methods, respectively. Prior to measurements, the catalysts were outgassed ex situ under vacuum at 180 °C for 20−24 h in a Micromeritics VacPrep 061 Sample Degas System followed by in situ outgassing for 4 h at 180 °C.

The amount and strength of Brønsted and Lewis acid sites were determined by Fourier transform infrared spectroscopy using pyridine (≥99.5%) as the probe molecule (with ATI Mattson FTIR Infinity Series spectrometer). The catalyst used in acidity measurements was calcined. The quantification of acid sites was performed using the molar extinction parameters reported by Emeis.[30]

Powder XRD patterns were obtained on a Bruker D8 Advance diffractometer (Cu K_α radiation, λ = 0.15418 nm) equipped with a LynxEye position sensitive detector. The data were collected in the 2θ range of 5°−65° with a step of 0.05° and a collection time of 3 s. The phase identification was performed using the ICDD PDF-2 database.[31] The average crystallite size of phases was calculated by the line broadening analysis according to the Scherrer equation. Scanning electron microscopy (SEM) was utilized to obtain information on the morphology of the binder, H-Beta-38, and the extruded catalysts. A Zeiss Leo Gemini 1530 microscope combined with secondary electron and backscattered electron detectors was applied. The X-ray analysis was performed with an acceleration voltage of 15 kV.

Transmission electron microscopy (TEM) was utilized to determine the metal particle size and study morphology and porosity. The equipment used for analysis was a JEM-1400Plus (JEOL, Japan) with a maximal acceleration voltage of 120 kV. The ImageJ program was used to interpret TEM images and determine particles sizes of the fresh and spent catalysts. Prior to the TEM measurements, the extrudates were ground and suspended in ethanol. A drop of a suspension was mounted on a copper grid coated with a carbon film, and the solvent evaporated. For calculation of the metal particle size distribution, the diameter (d) of more than 300 particles was determined in TEM micrographs.

Ni content was determined by inductively coupled plasma-optical emission spectroscopy (ICP-OES) using PerkinElmer Optima 5300 DV.

Hydrogen TPR experiments were performed with a Micromeritics Belcat II instrument. For a measurement, the catalyst was dried prior to an experiment under an argon flow using a temperature program of 25 °C-2 °C/min-120 °C (60 min). Thereafter, it was reduced using 5 vol % hydrogen in argon with the following temperature program: 25 °C-2 °C/min-350 °C (150 min). Hydrogen was analyzed using the thermal conductivity detector, and water was removed using a molecular sieve trap.

The mechanical strength of the extruded samples was estimated by the crush tester (SE 048, Lorentzen & Wettre) both in horizontal and vertical positions as it was described in

https://doi.org/10.1021/acs.iecr.2c02345
Ind. Eng. Chem. Res. 2022, 61, 12998−13010

Table 1. Ni Content for Fresh and Spent Composite Catalysts Determined by ICP Analysis and Textural Properties of Powder Clay and Extrudates[c]

			extrudates				
entry	sample	Ni content [wt %]	S_{BET} [m^2/g]	S_{DR} [m^2/g]	V [cm^3/g]	V_m/V_μ	D_{pore} [nm]
1	H-Beta-38[20]	n.d.	n.a.	590	0.31	0.35	0.67
2	attapulgite (powder)	n.d.	103	117	0.25	6	n.d.
	attapulgite (extrudate)	n.d.	97	116	0.37	12	n.d.
3	[Ni/(H-Beta-38+Att.)]	5.1	404	528	0.39	0.73	n.d.
4	[Ni/(H-Beta-38+Att.)] spent[a]	n.a.	206	267	0.23	1.07	n.d.
5	[(Ni/H-Beta-38)+Att.]	5.1	304	407	0.31	0.80	0.66
6	[(Ni/H-Beta-38)+Att.] spent[b]	4.8	193	246	0.22	1.20	0.63
7	[(Ni/Att.)+H-Beta-38]	4.8	355	460	0.32	0.63	0.66
8	[(Ni/Att.)+H-Beta-38] spent[b]	4.2	177	219	0.18	1.1	0.63

[a]This catalyst was used first in citronellal transformation; thereafter, it was reduced in situ and used in citral transformation. [b]These catalysts were only used in citral transformation. [c]A − specific surface area (BET: Brunauer−Emmett−Teller, DR: Dubinin-Radushkevich), V − pore volume (m: meso, μ: micro). n.d. not determined, n.a. not available.

Table 2. Brønsted and Lewis Acid Sites of Clay Materials

		BAS [μmol/g]				LAS [μmol/g]					
no.	sample	w	m	s	$\sum$	W	m	s	$\sum$	TAS [μmol/g]	BAS/LAS
1	attapulgite	1	5	0	6	27	8	0	34	40	0.2
2	H-Beta-38	17	40	221	278	19	10	2	31	309	9
3	70 wt % H-Beta-38 + 30 wt % Att.[a]	12	29	155	196	21	9	1	31	186	6
4	70 wt % H-Beta-38 + 30 wt % Att.[b]	15	45	42	102	39	20	9	68	170	1.5
5	[Ni/(H-Beta-38+Att.)]	13	19	35	67	96	33	26	155	222	0.43
6	[(Ni/H-Beta-38)+Att.]	25	22	68	115	97	27	43	167	282	0.69
7	[(Ni/Att.)+H-Beta-38]	9	48	44	101	62	38	9	109	210	0.93
8	[Ni/(H-Beta-38+Att.)] spent	10	6	17	91	7	3	8	115	206	0.79
9	[(Ni/Att.)+H-Beta-38] spent	14	72	17	103	44	31	5	80	183	1.29

[a]Theoretical value calculated as the weight-average. [b]Measured.

our previous publications.[32] For, e.g., the vertical crushing test, the cylindrical extrudate with a diameter of 1.4 mm and a length of 10 mm was inserted in between the two anvils of the crush tester, and then the load was applied along the vertical direction of the extrudate until it exhibited a failure. The maximum applied load was recorded, and after 10 extrudates were measured, the average value of their maximum applied loads was calculated as the sample mechanical strength.

2.3. Catalyst Testing. The experiments were carried out in a continuous trickle bed reactor (the internal diameter 1.25 cm, the reactor volume ∼ ca. 15 cm^3).[18] Quartz wool was placed at the bottom of the reactor followed by 1 g of extrudates. The inert quartz beads of the size 0.2−0.8 mm (∼15 g) were placed into the voids completely filling the reactor. The citronellal (Sigma-Aldrich, ≥95.0 wt %) and citral (cis/trans isomer ∼1/1, ≥95.0%, Sigma-Aldrich) solution in cyclohexane (0.086 M) was fed into the reactor with a feeding rate varying in the range of 0.2−0.4 mL min^{-1}, while the hydrogen flow rate was 100 mL min^{-1}.

Analysis of the reaction components was carried out using an Agilent GC 6890 N supplied with a DB-1 column (30 m × 250 μm × 0.5 μm), FID (340 °C). The temperature program included two steps: 1) from 110 to 130 °C with the temperature ramp of 0.4 °C min^{-1} and 2) from 130 to 200 °C with a temperature ramp of 13 °C min^{-1}. Identification of the reaction compounds was carried out by GC/MS with an Agilent GC/MS 6890 N/5973 using the same temperature program and column. Before analysis, the samples were diluted with cyclohexane (solvent) according to the procedure described in ref 18.

3. RESULTS AND DISCUSSION

3.1. Catalyst Characterization. Attapulgite exhibits according to the elemental analysis the SiO_2/Al_2O_3 ratio of 9 with the following amounts of different elements: 22 wt % Si, 5 wt % Al, and 6 wt % Mg as well as 2 wt % Fe, 1 wt % Ca, 0.2 wt % P, and 0.5 wt % K. This is in accordance with the results of ref 29 also reporting that attapulgite typically contains besides silica also rather large amounts of Mg(II), Al(III), and Fe(III).

The results from Ni content determination by ICP in the fresh and spent extrudates showed that Ni leaching was 5.9% from the initial Ni content in the spent [(Ni/H-Beta-38)+Att.], while it was 12.5% from the spent [(Ni/Att)+H-Beta-38] catalyst indicating weaker interactions of Ni with attapulgite in comparison to H-Beta-38 (Table 1).

The specific surface areas and the pore sizes were determined for H-Beta and attapulgite as well as for three composite catalysts (Table 1). The BET specific surface area of attapulgite is 103 m^2/g_{cat} which is quite close to the one reported in ref 33. Furthermore, the ratio between its meso- and micropores was 12, while it was 16.8 in ref 33. In addition, the Dubinin−Radushkevich method (DR) method was also used to estimate the specific surface area and the pore size (Table 1). The BET specific surface area of attapulgite in ref 23 was slightly higher, 188 m^2/g_{cat}; however, the origin of attapulgite was not given.

In Ni extrudates, a fully comparative analysis of the fresh and spent catalysts was done for [(Ni/H-Beta-38)+Att.] and [(Ni/Att.)+H-Beta-38] which were both applied in citronellal and citral transformations. The former spent catalyst exhibited 60%

https://doi.org/10.1021/acs.iecr.2c02345
Ind. Eng. Chem. Res. 2022, 61, 12998−13010

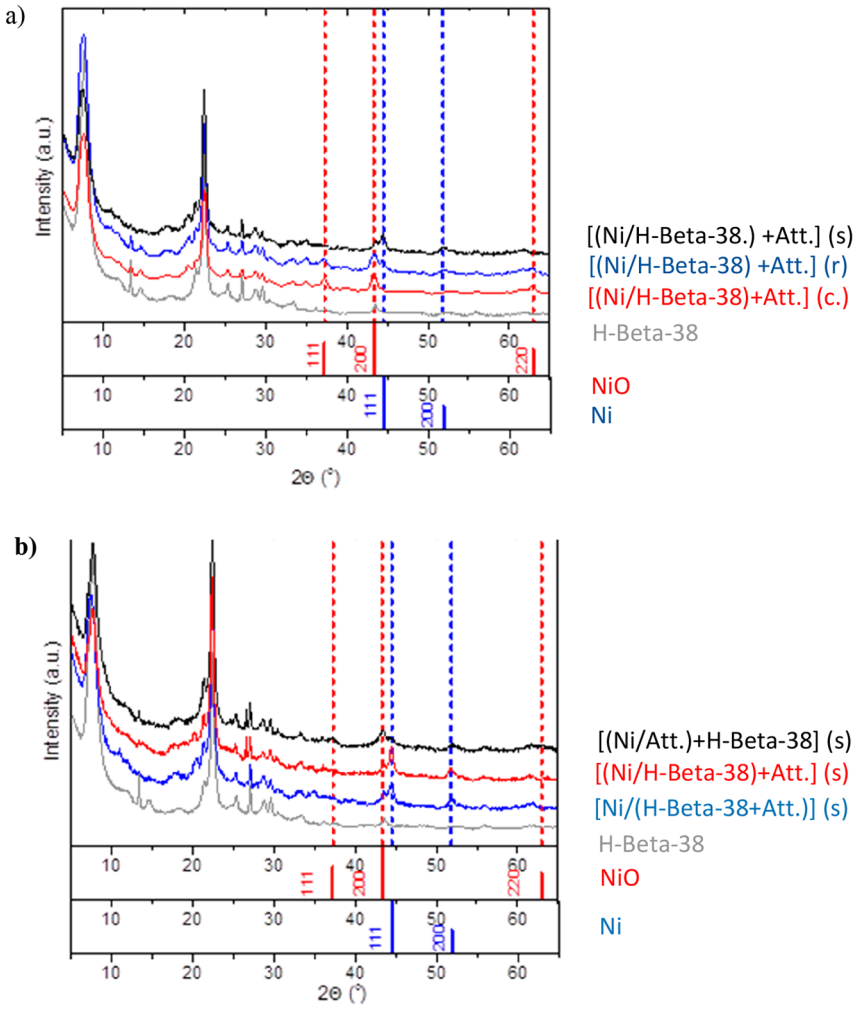

Figure 2. XRD patterns of **a)** the calcined (c.), freshly reduced (r), and spent (s) [Ni/(H-Beta-38+Att.)] extrudates compared to the initial H-Beta-38 zeolite and **b)** the spent [Ni/(H-Beta-38+Att.)], [(Ni/H-Beta-38)+Att.], and [(Ni/Att.)+H-Beta-38] extrudates compared to the initial H-Beta-38 zeolite. Notation: spent [Ni/(H-Beta-38+Att.)] was used first in citronellal transformation; thereafter, it was reduced in situ and used in citral transformation, while spent [(Ni/H-Beta-38)+Att.] and [(Ni/Att.)+H-Beta-38] extrudates were only used in citral transformation.

of the specific surface area of the fresh one determined by the DR method, while for [(Ni/Att.)+H-Beta-38], the corresponding value was only 48%. Analogous trends were observed for a decrease in the pore volume. These results indicate clearly that the catalyst with weaker interactions between the metal and the acid sites, when Ni is loaded on attapulgite, was deactivated more extensively than the one with Ni located on H-Beta-38. This result is also in accordance with the catalytic results for citral transformation (see below).

The amount of Brønsted and Lewis acid sites as well as their strengths is given in Table 2. Attapulgite exhibits only mild acidity, and no strong acid sites were present (Table 2). The absence of strong acid sites in the clay material can be attributed to the weak framework interactions of tetrahedral aluminum species. On the contrary, 6-fold more Lewis than Brønsted acid sites were observed for attapulgite. When calculating the acidity for 70% H-Beta-38−30 wt % attapulgite and comparing these values with the measured sample (Table 2, entries 3 and 4), it can be seen that although the total acidities were close to each other, the amount of Brønsted acid sites was decreased, and the opposite was observed for Lewis acid site concentration in the real sample showing that the acidity is not a linear function on composition. The most acidic extrudates were [Ni/(Beta-38+Att.)] followed by [(Ni/Beta-38+Att.)], and the lowest total acidity was obtained for [(Ni/Att.)+Beta-38]. When, however, the Ni precursor was first loaded on H-Beta-38 and then extruded, it exhibited a lower BAS/LAS ratio than the one in which Ni was loaded simultaneously on both H-Beta-38 and attapulgite. This result indicates that Ni blocked some acidic sites on H-Beta-zeolite. Interestingly also the BAS/LAS ratio was enhanced in the spent catalyst. It should be pointed out here that the measured amount of Lewis acid sites might be slightly higher in the calcined catalysts than those reduced and used in the reaction in the presence of metallic nickel, because it is known that metal oxides exhibit Lewis acidity.[34,35] However, for the comparative purposes, the same type of methodology was used for determination of acidity as in ref 20.

The most acidic catalyst was the one in which Ni was first supported on H-Beta-38 and then extruded with 30 wt % attapulgite followed by the catalyst when Ni was deposited on a composite extrudate [Ni/(H-Beta-38+Att.)], while the lowest acidity was recorded for [(Ni/Att.)+H-Beta-38]. On the other hand, the highest Brønsted to Lewis acid ratio (BAS/LAS) was observed for the latter catalyst with a small amount of H-Beta-38.

https://doi.org/10.1021/acs.iecr.2c02345
Ind. Eng. Chem. Res. 2022, 61, 12998−13010

Calcined, freshly reduced, and spent [Ni/(H-Beta-38+Att.)], [(Ni/H-Beta-38)+Att.], and [(Ni/Att.)+H-Beta-38] extrudates were studied by powder X-ray diffraction (Figure S2, Figure 2).

The XRD patterns of the reduced and spent [Ni/(H-Beta-38+Att.)] compared to the XRD patterns of the zeolite and calcined nonreduced [Ni/(H-Beta-38+Att.)] are depicted in Figure 2a.

The XRD pattern of the reduced [Ni/(H-Beta-38+Att.)] catalyst contains peaks from the phase of metallic nickel Ni^0 (PDF No. 04-0850, $a = b = c = 3.524$ Å) with an average CSD size $D_{Ni} = 14.5$ nm (Table 3, entry 2); the determined value of the lattice parameter is $a = 3.524$ Å. The XRD pattern of the sample also contains peaks from the nickel oxide phase NiO (PDF No. 047-1049, $a = b = c = 4.177$ Å) with an average CSD size $D_{NiO} = 11.5$ nm; the determined value of the lattice parameter is $a = b = c = 4.181$ Å. This lattice parameter is slightly larger than the one for the corresponding calcined sample (Table 3, entries 1, 2) which has also a smaller NiO particle size. This result is in accordance with thermodynamics, because the lattice size increases with a decreasing particle size due to the combined higher interfacial energy and mutual surface tension attractions of the smaller particles.[36] Additional peaks in the region of $2\theta = 20$ and 35° are attributed to the presence of magnesium silicate phases, characteristic for attapulgite $Mg_4Si_6O_{15}(OH)_2(H_2O)_6$ (PDF No. 04-016-3203) and mixed silicate $MgAlSi_4O_{10}(OH)(H_2O)_4$ (PDF No. 04-013-5980). It is worth noting that the spent [Ni/(H-Beta-38+Att.)] catalyst contains only the Ni^0 phase with the CSD size $D_{Ni} = 13.0$ nm (Table 3, entry 3), while the presence of the nickel oxide phase is not observed indicating that in situ reduction of surface nickel species into the zero valence state was efficient.

Table 3. NiO and Ni Particle Sizes Determined by XRD and TEM[b]

		XRD				TEM
entry	sample	D_{NiO} (nm)	a (Å)	D_{Ni^0} (nm)	a (Å)	D (nm)
1	[Ni/(H-Beta-38+Att.)] calcined	18.0	4.180	n.d.	n.d.	n.d.
2	[Ni/(H-Beta-38+Att.)] reduced	11.5	4.181	14.5	3.524	n.d.
3	[Ni/(H-Beta-38+Att.)] spent	n.d.	n.d.	13.0	3.523	n.d.
4	[(Ni/H-Beta-38)+Att.] calcined	19.0	4.180	n.d.	n.d.	n.d.
5	[(Ni/H-Beta-38)+Att.] reduced	n.d.	n.d.	n.d.	n.d.	9.8
6	[(Ni/H-Beta-38)+Att.] spent	n.d.	n.d.	18.0	3.524	n.d.
7	[(Ni/Att.)+H-Beta-38] calcined	12.0	4.178	n.d.	n.d.	n.d.
8	[(Ni/Att.)+H-Beta-38] reduced	n.d.	n.d.	n.d.	n.d.	6.2[a]
9	[(Ni/Att.)+H-Beta-38] spent	10.0	4.182	9.0	3.524	n.d.

[a]Difficult to separate nickel and impurity particles in attapulgite. [b]Spent [Ni/(H-Beta-38+Att.)] was used first in citronellal transformation; thereafter, it was reduced in situ and used in citral transformation, while the spent [(Ni/H-Beta-38)+Att.] and [(Ni/Att.)+H-Beta-38] extrudates were only used in citral transformation. n.d. not determined.

The powder XRD patterns of all spent catalysts, [Ni/(H-Beta-38+Att.)], [(Ni/H-Beta-38)+Att.], and [(Ni/Att.)+H-Beta-38] extrudates, and that of the initial H-Beta-38 zeolite are shown in Figure 2b. According to XRD data, all samples contain the characteristic peaks of the H-Beta-38 zeolite. A narrow maximum at $2\theta = 26.6°$ observed for [Ni/(H-Beta-38+Att.)] and [(Ni/Att.)+H-Beta-38] extrudates was also present in XRD patterns of the corresponding calcined samples (Figure S2), which can be related to the SiO_2 quartz phase (PDF No. 00-046-1045) with the CSD size $D_{SiO2} > 100$ nm. The zeolite material in the spent samples undergoes minor structural changes during the reaction as indicated by a slight decrease in the intensity of the peaks at 2θ at 7.7 and 13.4°. Additional peaks in the 2θ region of 20° and 35° in the spent [Ni/(H-Beta-38+Att.)] and [(Ni/H-Beta-38)+Att.] similar to that observed in the corresponding nonreduced calcined extrudates are attributed to the presence of magnesium silicate phases. In the spent catalysts where nickel was supported on the zeolite or the zeolite was mixed with attapulgite, [Ni/(H-Beta-38+Att.)], and [(Ni/H-Beta-38)+Att.], only the metallic nickel phase Ni^0 was recorded with the corresponding CSD size $D_{Ni} = 13.0$ nm and $D_{Ni} = 18.0$ nm (Table 3, entries 3 and 6), respectively, indicating rather high resistance of the active metal sites to oxidation under reaction conditions. The determined values of the Ni^0 lattice parameters for [Ni/(H-Beta-38+Att.)] and [(Ni/H-Beta-38)+Att.] are 3.523 and 3.524 Å, respectively. In the XRD pattern of the sample where Ni was supported on attapulgite [(Ni/Att.)+H-Beta-38], weak peaks from the phase of metallic nickel Ni^0 (PDF No. 04-0850) are observed with the estimated CSD size $D_{Ni} = 9.0$ nm (Table 3, entry 9) and the determined value of the lattice parameter of 3.524 Å. Along with metallic nickel Ni^0 there is also the nickel oxide phase NiO (PDF No. 047-1049) with the determined value of the lattice parameter $a = b = c = 4.182$ Å and an average CSD size $D_{NiO} = 10.0$ nm. The larger lattice parameter of the NiO phase in the spent [(Ni/Att.)+H-Beta-38] together with its smaller NiO size in comparison to the one detected in thermodynamics analogously is observed for the NiO phase in calcined and reduced [(Ni/H-Beta-38)+Att.]. The fraction of the nickel oxide phase in [(Ni/Att.)+H-Beta-38] noticeably dominates over the metallic nickel phase (Figure 5) which can result in its lower hydrogenation ability compared to [Ni/(H-Beta-38+Att.)] and [Ni/H-Beta-38+Att.] characterized by the presence of only the metallic nickel phase.

TEM images of attapulgite, H-Beta-38 and the three different Ni-H-Beta-attapulgite extrudates are shown in Figure 3. Attapulgite has a typical fibrous structure, with some metal particles as impurities (Figure 3a). Attapulgite fibers have a diameter of ca. 25 nm with their lengths varying from 115 to 1200 nm. The size of the metal particles in pure attapulgite is ca. 45 nm. H-Beta-38 has round shaped crystals with the size of 125 nm (Figure 3b). Because pure commercial attapulgite has also metal particles, it is challenging to determine Ni particle size distribution in [Ni/(H-Beta-38+Att.)] and in [(Ni/Att.)+H-Beta-38] (Figure 3c, e). On the other hand, when Ni was first introduced on H-Beta-38, the average Ni particle size can be reliably determined as being 9.8 nm (Figure 3b, Table 3, entry 5).

The Ni particle size distribution can be correctly calculated from TEM only for [(Ni/H-Beta-38)+Att.], because Ni was only loaded on round shaped H-Beta particles (Figure 4a) and thereafter dried, calcined, extruded with attapulgite, and

https://doi.org/10.1021/acs.iecr.2c02345
Ind. Eng. Chem. Res. 2022, 61, 12998−13010

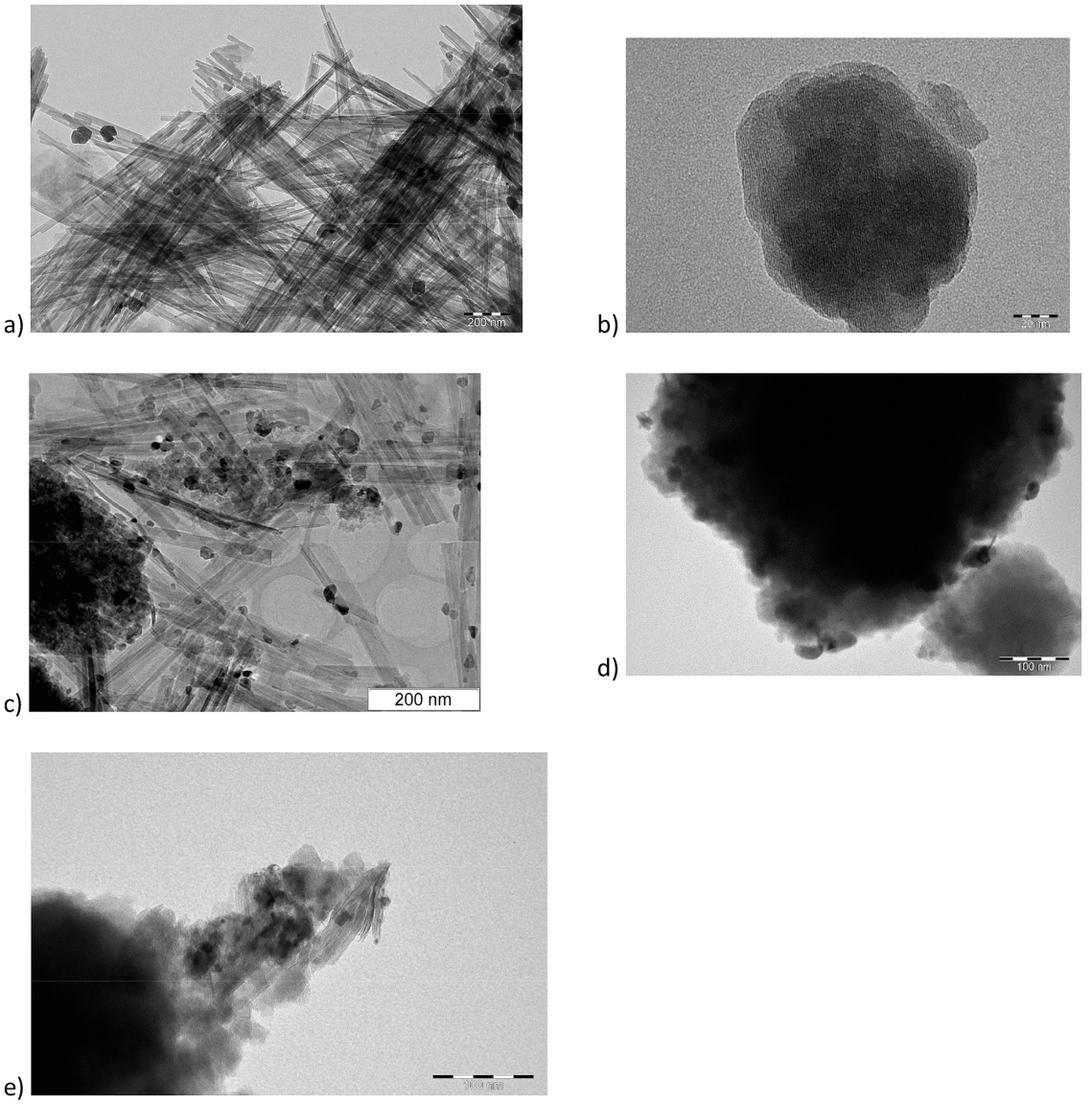

Figure 3. TEM images of a) attapulgite, b) H-Beta-38, c) [Ni/(H-Beta-38+Att.)], d) [(Ni/H-Beta-38)+Att.], and e) [(Ni/Att.)+H-Beta-38].

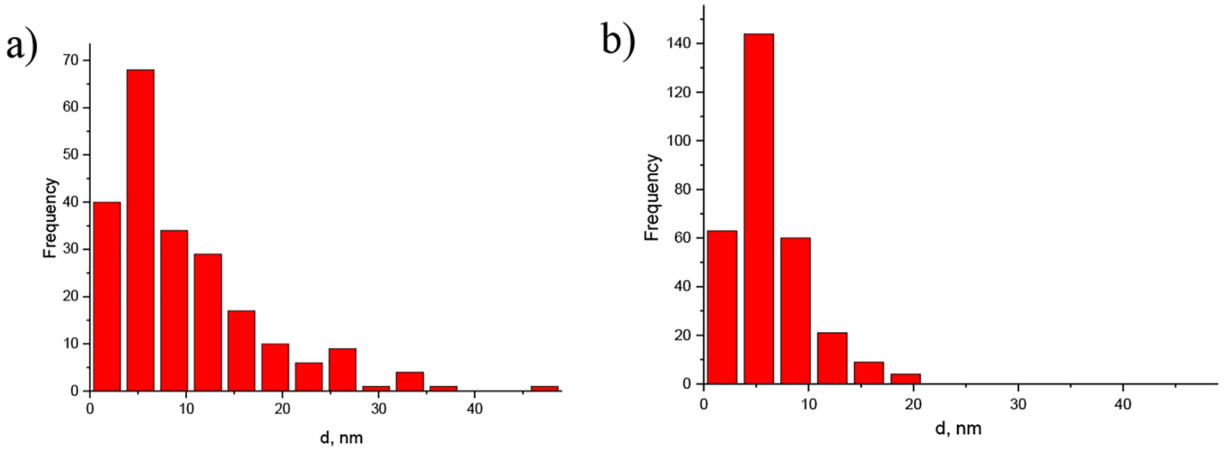

Figure 4. Metal particle size distribution determined by TEM for a) [(Ni/H-Beta-38)+Att.] and b) [(Ni/Att.)+H-Beta-38].

reduced. On the other hand, when Ni was loaded for both Beta-30 and attapulgite, Ni particle size distribution cannot be reliably calculated on the attapulgite phase, because Ni particles cannot be clearly differentiated with the impurities present in attapulgite phase. In this case, the particles on attapulgite can be either Ni and other impurities present in

https://doi.org/10.1021/acs.iecr.2c02345
Ind. Eng. Chem. Res. 2022, 61, 12998−13010

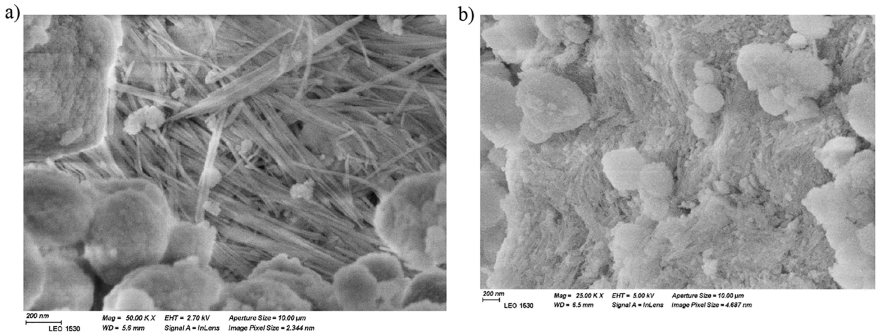

Figure 5. SEM images of the fresh, reduced a) [(Ni/H-Beta-38)+Att.] and b) [(Ni/Att.)+H-Beta-38] catalysts.

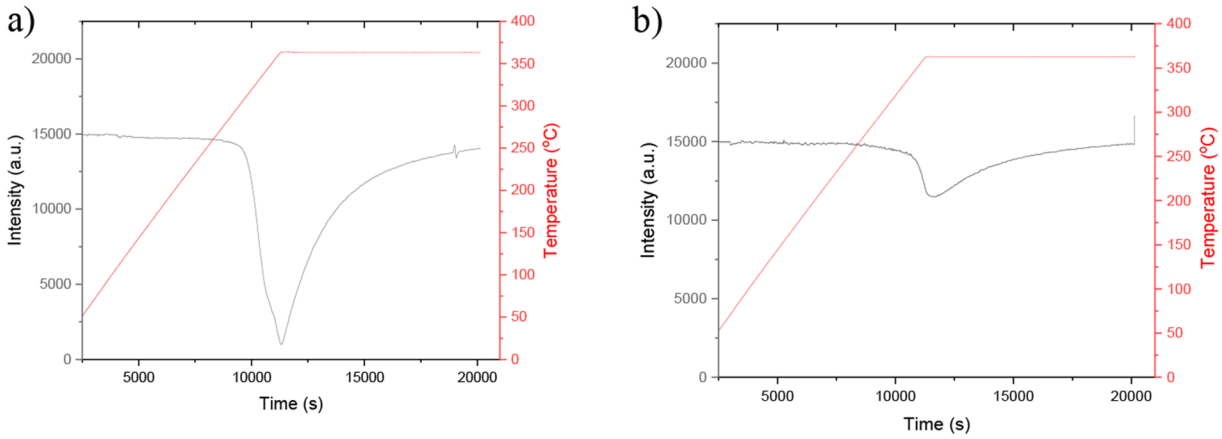

Figure 6. Hydrogen TPR of a) [(Ni/H-Beta-38)+Att.] and b) [(Ni/Att.)+H-Beta-38].

attapulgite. The average Ni particle size for reduced [(Ni/H-Beta-38)+Att.] was 9.8 nm (Table 3, entry 5, Figure 4a). The average particle size of Ni for the spent [(Ni/H-Beta-38)+Att.] determined by XRD was 18 nm indicating that some sintering might occur (Table 3, entry 6). However, typically the metal particle size determined by XRD can be larger than determined by TEM, because XRD cannot detect clearly particles below ca. 3 nm.

SEM images of fresh, reduced [(Ni/H-Beta-38)+Att.] and [(Ni/Att.)+H-Beta-38] show that when Ni was first loaded on H-Beta-38 and thereafter extruded with attapulgite, the fibers were more clearly separated (Figure 5a), while in the latter catalyst, attapulgite fibers are more bound together (Figure 5b).

Hydrogen temperature-programmed reduction was performed to reveal hydrogen consumption dependency on temperature. Two different Ni extrudate catalysts, [(Ni/H-Beta-38)+Att.] and [(Ni/Att.)+H-Beta-38], were reduced similarly prior to the experiment, i.e., 2 °C/min ramping rate up to 350 °C and holding at that temperature for 150 min. The results from the temperature-programmed reduction revealed that the maximum hydrogen uptake for both catalysts occurs at 350 °C (Figure 6). For the former catalyst, a rapid hydrogen consumption started already at 305 °C, while for [(Ni/Att.)+H-Beta-38], reduction of NiO started more rapidly at 348 °C. Furthermore, the total area from hydrogen consumption was 4.2-fold higher for [(Ni/H-Beta-38)+Att.] in comparison to the one where Ni was deposited on attapulgite. This result indicates that it is easier to reduce nickel deposited on Beta-zeolite. As a comparison with the literature, Ni/H-Beta with the Ni particle size of 19.1 nm exhibited the lowest hydrogen consumption at 405 °C, when the TPR heating rate of 10 °C/min was used.[37] Furthermore, for Ni/attapulgite calcined at 500 °C, the reduction of NiO started already at 328 °C indicating reduction of isolated, free NiO particles exhibiting weak interactions with the support.[38]

The mechanical strength of extrudates consisting of Beta-38 and attapulgite before Ni deposition was determined to be 3.3 ± 0.5 and 2.6 ± 0.1 MPa in the vertical and horizontal positions, respectively (Table 4, entry 1). After Ni introduction, the mechanical strength was slightly increased to 4.5 ± 0.5 and 3.3 ± 0.1 MPa in the vertical and horizontal positions, respectively (Table 4, entry 2). A slightly higher value for [Ni/(H-Beta-38+Att.)] extrudates compared to the metal-free composite (H-Beta-38+Att.) can be attributed to the reinforcing effect of the metallic Ni on the extrudate structure. These values are relatively high compared to the mechanical strength of Ni supported on mesoporous alumino silicate-sepiolite extrudates earlier applied for citral hydrogenation[20] (3.2 ± 0.7 and 0.4 ± 0.1 MPa in the vertical and

Table 4. Average Mechanical Strength of Extrudates in Vertical and Horizontal Positions

no.	sample	mechanical strength (vertical), MPa	mechanical strength (horizontal), MPa
1	Beta-38 + attapulgite	3.3 ± 0.5	2.6 ± 0.8
2	Ni/(Beta-38 + attapulgite)$_{spent}$	4.5 ± 0.5	3.3 ± 0.9
3	attapulgite[29]	16.3 ± 1.6	7.7 ± 0.8
4	sepiolite[29]	5.6 ± 0.6	3.5 ± 0.4

https://doi.org/10.1021/acs.iecr.2c02345
Ind. Eng. Chem. Res. 2022, 61, 12998−13010

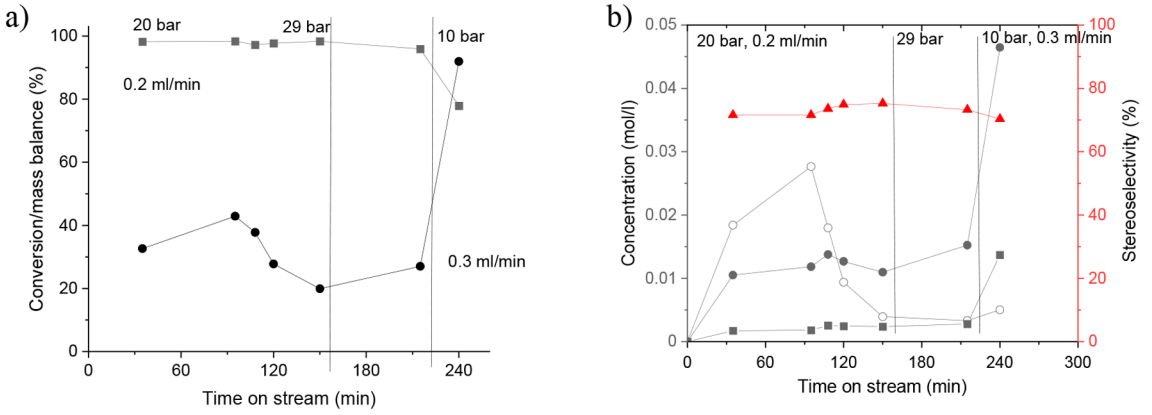

Figure 7. a) Conversion of citronellal (■) and liquid phase mass balance (●) and b) concentration of menthols (●), acyclic hydrogenation products (■), and defunctionalized products (○) and stereoselectivity to menthol (Δ) in citronellal transformation over [Ni/(H-Beta-38+Att.)] as a function of TOS. The liquid flow rate was 0.2 mL/min during 215 min TOS; thereafter, it was 0.3 mL/min.

horizontal positions, respectively). It should be noted that pure attapulgite extrudates exhibited higher mechanical strength of 16.3 ± 1.6 and 7.7 ± 0.8 MPa in vertical and horizontal positions,[29] respectively (Table 4, entry 3), than neat sepiolite extrudates (5.6 ± 0.6 and 3.5 ± 0.4 MPa in vertical and horizontal positions,[29] respectively) (Table 4, entry 4) indicating higher intrinsic endurance of attapulgite-containing extrudates.

3.2. Catalytic Results on Menthol Synthesis. Citronellal transformations were initially performed with the catalyst where Ni was deposited on both the zeolite and the binder, [Ni/(H-Beta-38+Att.)]. During the first 240 min, TOS citronellal disappeared from the bulk liquid either because of the reaction or strong adsorption on the catalyst surface giving citronellal conversion of ca. 95−98%. The liquid phase mass balance closure, which is the sum of the unconverted reactant and products visible in GC analysis of the liquid phase, was only between 20 and 40% within this time period. When using a higher liquid flow rate of 0.3 mL/min, the liquid mass balance increased to 92%. Thus, for citral transformations at a higher liquid flow rate, 0.3 mL/min was used (see below).

The main products initially up to 108 min TOS were p-menthanes, which were formed by dehydration of menthols due to too high Brønsted acidity of the catalyst analogous to dehydration of 1-phenylethanol.[39] When the most acids sites were, however, deactivated, the yield of menthols still remained constant when using the low liquid flow rate of 0.2 mL/min (Figure 7b). When, however, the liquid flow rate was increased to 0.3 mL/min, both the liquid phase mass balance closure and the yields of menthol and acyclic hydrogenation products increased. Maximally, the menthol yield of 53% was obtained at TOS of 240 min over [Ni/(H-Beta-38+Att.)]. Stereoselectivity to menthols was in the range of 70−75% remaining rather constant with increasing time-on-stream. As a comparison, the menthol yield from citronellal over [Ni/(H-Beta-38+Sep.)] was 44% in a trickle bed reactor,[20] which is lower than in the current case with [(Ni/H-Beta-38+Att.)]. On the other hand, stereoselectivity to menthol over both catalysts was ca. 71−76% being thus unaffected by the BAS/LAS ratio. Ni extrudates exhibited also selectivity to menthol in citronellal transformations in a trickle bed reactor higher than several Pt- and Ru-H-Beta-zeolite-bentonite extruded catalysts studied previously also in a fixed bed continuous reactor.[5]

Citral transformations over three different Ni-H-Beta-38-attapulgite extrudates, in which Ni is located on Beta-38 [(Ni/H-Beta-38)+Att.], on attapulgite [(Ni/Att.)+H-Beta-38], and on both of them [Ni/(H-Beta-38+Att.)], demonstrated the highest conversion when Ni was supported on the acidic Beta-38 zeolite with attapulgite as a binder (Figure 8a). The composite catalyst [Ni/(H-Beta-38+Att.)] used in citronellal transformation was reduced in situ at 350 °C for 2.5 h with hydrogen, while the two others were freshly reduced catalysts. This apparently should be taken into account while comparing catalytic behavior of these materials.

A slightly lower conversion was obtained when nickel was located both on Beta-38 and attapulgite in comparison to [(Ni/H-Beta-38)+Att.], while the lowest conversion was detected when nickel was deposited on attapulgite indicating that the proximity of the acid and metal sites is essential for efficient catalytic behavior. When the pressure was decreased after 180 min time-on-stream to 15 bar, citral conversion decreased linearly with the two most active catalysts (Figure 8a). No sintering occurred for [Ni/(H-Beta-38+Att.)] based on XRD measurements (Table 3) indicating that Ni is more strongly bound on Beta-38 than on attapulgite. On the other hand, activity decline with nickel deposited on attapulgite being significant at 20 bar during 180 min TOS was much less pronounced at 15 bar total pressure.

The reactant is supplied as a mixture of cis and trans isomers with potentially different reactivity. The cis/trans ratio of citral was rather constant with time-on-stream at different pressures. It was, however, the highest with the most acidic catalyst and the lowest one over the catalyst in which Ni is located on mildly acidic attapulgite (Figure 8b). With the most acidic catalyst, the cis/trans ratio increased rapidly with TOS under 20 bar to 1.47; thereafter, it was ca. 1.2−1.3. This result indicated that *trans*-citral reacted faster under mass transfer limitations, which is in line with the results obtained previously in a trickle bed reactor for Ru-/H-Y extrudates.[17] However, in that case,[17] this ratio decreased with increasing time-on-stream. In a study performed in a batch reactor under kinetic regime over Ni/MCM-41,[14] it was observed that *cis*-citral reacted initially faster than *trans*-citral. On the other hand, the cis/trans ratio decreased from the initial value of 0.33 to 0.23 and remained unchanged after a 15 min reaction time indicating that *trans*-citral reacted faster upon catalyst deactivation, which

https://doi.org/10.1021/acs.iecr.2c02345
Ind. Eng. Chem. Res. 2022, 61, 12998−13010

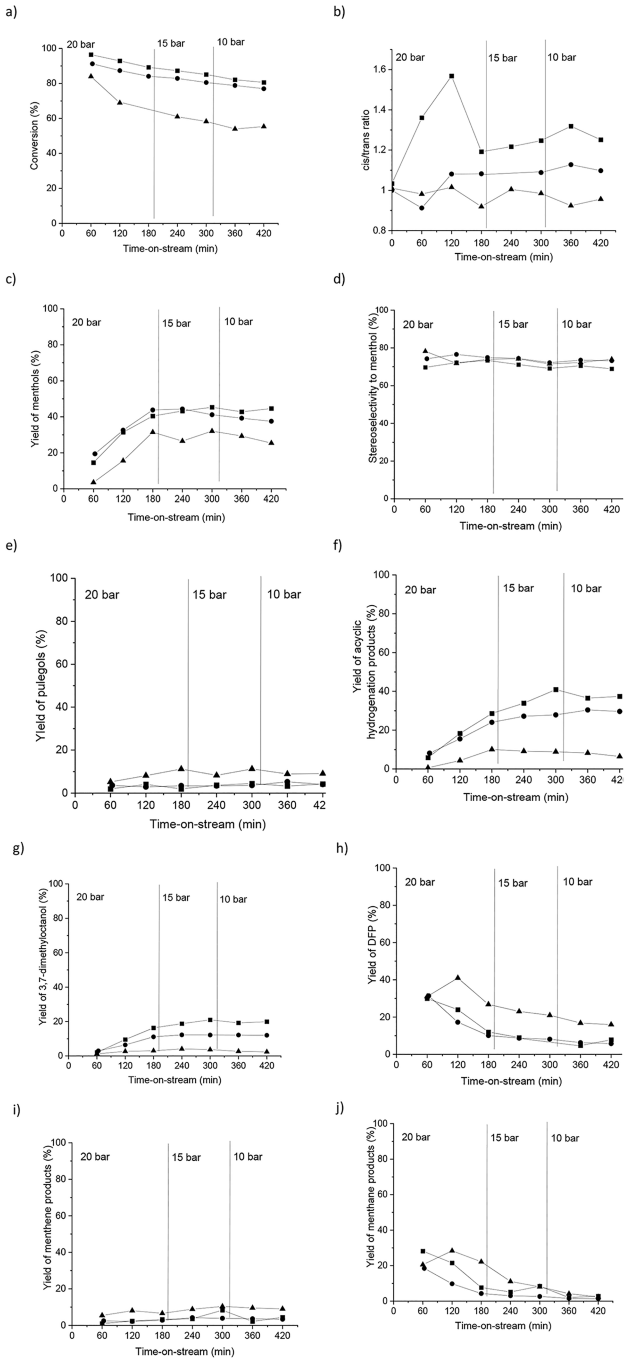

Figure 8. a) Conversion of citral, b) cis/trans ratio of citral, c) yield of menthols, d) stereoselectivity to menthol, e) yield of pulegols, f) acyclic hydrogenation products, g) 3,7-dimethyloctanol, h) defunctionalized products, (i) menthenes, and j) menthanes as a function of time-on-stream in citral transformation to menthols over different types of Ni extrudates. Notation: (■) [(Ni/H-Beta-38)+Att.], (●) [Ni/(H-Beta-38+Att.)], and (▲) [(Ni/Att.)+H-Beta-38].

might be due to the limited adsorption of the cis isomer on the coked surface.

Menthol yields increased with increasing TOS under 20 bar showing the slow reactor dynamics, when the steady state conditions were approaching during 180 min (Figure 8c). Thereafter, when the pressure was decreased to 15 bar, the menthol yields remained at about the same level for the subsequent 120 min TOS, while slightly lower menthol yields were obtained under 10 bar of total pressure at 360 min TOS. According to Nie et al.,[15] higher menthol yields were achieved under low total pressures in a batch reactor. In the current case, however, the most acidic sites of the catalyst have already been deactivated increasing the menthol selectivity at high TOS. Such an increase came at the expense of defunctionalized products (see below) formed by dehydration of menthol.[37,39]

The highest yields of menthols were obtained with Ni extrudates which exhibited the highest acidity, i.e., [(Ni/H-Beta-38)+Att.] (45%) and [Ni/(H-Beta-38+Att.)] (44%), respectively, while the lowest ones were demonstrated for [(Ni/Att.)+H-Beta-38] (Figure 8c). These two catalysts exhibited rather high amounts of strong Lewis acid sites (Table 2) which, according to Chuah et al.,[40] along with weak Brønsted acidity are beneficial for cyclization of citronellal. Menthol formation remained stable over [(Ni/H-Beta-38)+Att.] after 360 min TOS, while with the two other catalysts, it decreased continuously. Stereoselectivity to the desired menthol isomer was stable as a function of TOS being in the range of 68−78% (Figure 8d). Note that Ni particle size for [(Ni/H-Beta-38)+Att.] is 9.8 nm giving menthol selectivity of 44%, while it was 8 nm for Ni supported on a mesoporous alumino-silicate-sepiolite composite catalyst[21] with the corresponding maximum menthol selectivity of 75%. This result shows that although Ni particle sizes were quite close to each other, the maximum menthol selectivity was much higher in the latter case. This catalyst, the Ni supported on mesoporous alumino-silicate-sepiolite composite catalyst, exhibited no strong Brønsted acid sites, while [(Ni/H-Beta-38)+Att.] contained 68 μmol/g_{cat} them (Table 2, entry 6) indicating the undesired effect of strong Brønsted acid sites on menthol selectivity. The yields of pulegols were higher over [(Ni/Att.)+H-Beta-38] in comparison with the two more active catalysts, [Ni/(H-Beta-38+Att.)] and [(Ni/H-Beta-38)+Att.]. Selectivity to the desired menthol isomer increased with decreasing conversion (Figure 8a), which declined with TOS due to catalyst deactivation. However, at a certain TOS, menthol selectivity decreased for [(Ni/Att.)+H-Beta-38] as well as for [Ni/(Beta-38+Att.)] with decreasing conversion, while for [(Ni/H-Beta-38)+Att.], it remained constant. It is also clearly visible in Figure 8a that at the same conversion level [(Ni/Att.)+H-Beta-38] exhibited the lowest selectivity to the desired menthol also suffering from rapid deactivation, because the metallic nickel was easily oxidized in this catalyst based on XRD measurements (Figure 5). As a comparison to the literature, the highest menthol yield in a batch reactor was reported over 15 wt % Ni/Zr/MCM-41 when using a pressure ramp from 0.2−20 bar at 80 °C in *tert*-butanol as a solvent.[15] On the other hand, under isobaric conditions, the best performance was observed for 8 wt % Ni/H-MCM-41 giving a 94% menthol yield at 2 bar and 70 °C in toluene.[2] This catalyst contained only weak acid sites according to ammonia TPD. In addition, 75% selectivity of menthols at 98% citral conversion over 5 wt % Ni/mesoporous aluminosilicate-sepiolite extrudates [Ni/(MAS+sepiolite)] was reported in ref 21. When comparing the current results with [Ni/(Beta-38+Att.)] with 44−45% menthol yields, it can be observed that this catalyst contains a 2.23-fold higher amount of Brønsted acid sites[21] than (Ni/(MAS+sepiolite)). Furthermore, comparing the performance of [Ni/(H-Beta-38+Att.)] with that of [Ni/(H-Beta-38+Sep.)] in a trickle bed reactor under the same conditions, it can be stated that the maximum menthols were about the same, i.e., a 44% menthol yield was achieved in the

https://doi.org/10.1021/acs.iecr.2c02345
Ind. Eng. Chem. Res. 2022, 61, 12998−13010

current work, while the latter one in ref 20 gave the maximum menthol yield of 49%. Despite relatively high amounts of impurities in attapulgite, it was equally good as a binder as sepiolite with a much lower amount of impurities.[33] The corresponding Brønsted to Lewis acid ratio in [Ni/(H-Beta-38+Att.)] was 0.43, while for [Ni/(H-Beta-38+Sep.)], it was 0.63.[20] Moreover, the menthol yield decreased with increasing time-on-stream over [Ni/(H-Beta-38+Att.)] only by 19%, while for [Ni/(H-Beta-38+Sep.)], a corresponding decrease was ca. 30% due to its higher BAS/LAS ratio, showing the importance of the BAS/LAS ratio on catalyst stability. These results clearly show that the preparation method of the Ni-H-Beta-38-attapulgite composite catalyst is very important for menthol synthesis, and especially the metal location close to the acidic sites of zeolite is important. When Ni was originally loaded on mildly acidic attapulgite, it was not efficient, and the metallic nickel was not stable under reaction conditions.

The yield of acyclic hydrogenation products, citronellol and 3,7-dimethyloctanol, followed the patterns observed also for menthol formation indicating parallel formation of both menthols and acyclic hydrogenation products for all catalysts with different metal locations (Figures S3, S4). The lowest formation of acyclic hydrogenation products was observed for [(Ni/Att.)+H-Beta-38]. The yield of citronellol remained low, because it was hydrogenated rapidly to 3,7-dimethyloctanol. The amount of 3,7-dimethyloctanol was very high in the current work, especially for [(Ni/H-Beta-38)+Att.], which is opposite from those results obtained over Ni-MCM-41 in refs 14 and 16 in a batch reactor, where either no hydrogenation products and only traces of them were produced. In Ni-MCM-41, the BAS/LAS ratio was 0.52, while for [(Ni/H-Beta-38)+Att.], it was 0.69.

The highest yield of defunctionalized products (DFP), maximally 42% at 120 min TOS, was obtained over [(Ni/Att.)+H-Beta-38] (Figure 8h), which exhibited the lowest acidity, while the two other catalysts were active in hydrogenation. The yields of DFP decreased with increasing TOS due to catalyst deactivation. The main DFP products were menthanes (Figure 8j), which were formed in the second step after dehydration of menthol forming menthenes, followed by their hydrogenation. It can also be noticed that menthenes are not further hydrogenated on [(Ni/Att.)+H-Beta-38] due to severe catalyst deactivation (Figure 8i). As a comparison to the literature, maximally 22% DFP products were obtained over mildly acidic Ru/H-Y-80 extrudates using bindzil as a binder in a trickle bed reactor.[17] Analogously Ru-MCM-41 gave in a batch reactor an ca. 24% yield of DFP,[18] while an ca. 40% DFP yield was obtained over Ni-H-MCM-41.[16] As a comparison, the yield of DFP products over [Ni/(H-Beta-38+Att.)] was initially ca. 30%, while for [Ni/(H-Beta-38+Sep.)] with a higher BAS/LAS ratio, it was substantially higher 49%. However, with both catalysts, as expected, the DFP yield decreased to ca. 8% with increasing time-on-stream due to catalyst deactivation.

4. CONCLUSIONS

The one-pot synthesis of menthol was demonstrated in the current work in a continuous trickle bed reactor using three different types of Ni containing extrudates prepared on the basis of the H-Beta-38 zeolite and attapulgite as a binder with varying Ni locations. In the first catalyst, Ni is located both on Beta-38 and attapulgite [Ni/(H-Beta-38+Att.)], while in the two other catalysts, Ni was deposited on attapulgite [(Ni/Att.)+H-Beta-38] and on Beta-38 [(Ni/H-Beta-38)+Att.], respectively. These extrudates exhibited different acidity and metal dispersion, which was correlated with its catalytic performance. Maximally a 45% yield of menthol was obtained at 70 °C under 15 bar total pressure over Ni supported on H-Beta-38 followed by extrusion with attapulgite clay. In this catalyst, the proximity of Ni and acid sites facilitated the formation of menthol requiring a bifunctional catalyst. Citral conversion decreased slightly with increasing time-on-stream; however, the best catalyst exhibited also the lowest deactivation rate. The other main products under these conditions were 3,7-dimethyloctanol and menthanes with the yields of 20% and 22%, respectively. These products were formed, because the [(Ni/H-Beta-38)+Att.] catalyst exhibited suitable Ni particle size, ca. 10 nm, and rather high amounts of strong Brønsted acid sites. As a comparison, it can be stated that the [(Ni/H-Beta-38)+Att.] composite catalyst exhibited a similar performance as Ni-H-Beta-38 extruded with sepiolite clay, although the former clay contains also a higher amount of impurities. Furthermore, mechanical strength of [(Ni/H-Beta-38)+Att.] extrudates was rather high. As a comparison, very high initial selectivity to menthols was obtained in a previous work over Ni supported on mesoporous alumino-silicate sepiolite extrudates, which, however, was suffering rapid deactivation.

■ ASSOCIATED CONTENT

Supporting Information

The Supporting Information is available free of charge at https://pubs.acs.org/doi/10.1021/acs.iecr.2c02345.

Catalyst characterization: pore size distribution, XRD of extrudates. Catalytic data: selectivity to desired menthol as function of conversion, concentration of menthol vs concentration of 3,7-dimethyloctanol and their ratio vs conversion (PDF)

■ AUTHOR INFORMATION

Corresponding Author

Dmitry Yu. Murzin − *Åbo Akademi University, Johan Gadolin Process Chemistry Centre, 20500 Turku/Åbo, Finland;* orcid.org/0000-0003-0788-2643; Email: dmurzin@abo.fi

Authors

Irina L. Simakova − *Boreskov Institute of Catalysis, Novosibirsk, Russia 630090;* orcid.org/0000-0002-5138-4847

Päivi Mäki-Arvela − *Åbo Akademi University, Johan Gadolin Process Chemistry Centre, 20500 Turku/Åbo, Finland;* orcid.org/0000-0002-7055-9358

Mark Martínez-Klimov − *Åbo Akademi University, Johan Gadolin Process Chemistry Centre, 20500 Turku/Åbo, Finland*

Joseph Muller − *Åbo Akademi University, Johan Gadolin Process Chemistry Centre, 20500 Turku/Åbo, Finland*

Zuzana Vajglová − *Åbo Akademi University, Johan Gadolin Process Chemistry Centre, 20500 Turku/Åbo, Finland*

Markus Peurla − *Institute of Biomedicine, University of Turku, FI-20520 Turku, Finland*

Kari Eränen − *Åbo Akademi University, Johan Gadolin Process Chemistry Centre, 20500 Turku/Åbo, Finland*

Complete contact information is available at:

https://doi.org/10.1021/acs.iecr.2c02345
Ind. Eng. Chem. Res. 2022, 61, 12998−13010

https://pubs.acs.org/10.1021/acs.iecr.2c02345

Notes

The authors declare no competing financial interest.

■ ACKNOWLEDGMENTS

The authors are grateful to the Academy of Finland for funding through the following project: Synthesis of spatially controlled catalysts with superior performance. Electron microscopy samples were processed and analyzed in the Electron Microscopy Laboratory, Institute of Biomedicine, University of Turku, which receives financial support from Biocenter Finland. I.S. is grateful for the support from the Ministry of Science and Higher Education of the Russian Federation under the governmental order for the Boreskov Institute of Catalysis (project AAAA-A21-121011390055-8).

■ REFERENCES

(1) Patel, T.; Ishiuji, Y.; Yosipovitch, G. Menthol: a refreshing look at this ancient compound. *J. Am. Academy Dermat.* **2007**, *57* (5), 873−878.

(2) Trasarti, A. F.; Marchi, A. J.; Apesteguıa, C. R. Highly selective synthesis of menthols from citral in a one-step process. *J. Catal.* **2004**, *224*, 484−488.

(3) Vajglová, Z.; Kumar, N.; Peurla, M.; Eränen, K.; Mäki-Arvela, P.; Murzin, D. Yu. Cascade transformations of (±)-citronellal to menthol over extruded Ru-MCM-41 catalysts in a continuous reactor. *Catal. Sci. Techn.* **2020**, *10*, 8108−8119.

(4) Plößer, J.; Lucas, M.; Claus, P. Highly selective menthol synthesis by one-pot transformation of citronellal using Ru/H-BEA catalysts. *J. Catal.* **2014**, *320*, 189−197.

(5) Azkaar, M.; Mäki-Arvela, P.; Vajglová, Z.; Fedorov, V.; Kumar, N.; Hupa, L.; Hemming, J.; Aho, A.; Murzin, D. Yu. Synthesis of menthol from citronellal over supported Ru- and Pt-catalysts in continuous flow. *React. Chem. Eng.* **2019**, *4*, 2156−2169.

(6) Balu, A. M.; Campelo, J. M.; Luque, R.; Romero, A. A. One-step microwave-assisted asymmetric cyclisation/hydrogenation of citronellal to menthols using supported nanoparticles on mesoporous materials. *Org. Biomol. Chem.* **2010**, *8*, 2845−2849.

(7) Mertens, P.; Verpoort, F.; Parvulescu, A. N.; De Vos, D. Pt/H-beta zeolites as productive bifunctional catalysts for the one-step citronellal-to-menthol conversion. *J. Catal.* **2006**, *243*, 7−13.

(8) da Silva Rocha, K. A.; Robles-Dutenhefner, P. A.; Sousa, E. M. B.; Kozhevnikova, E. F.; Gusevskaya, E. Pd-heteropoly acid as a bifunctional heterogeneous catalyst for one-pot conversion of citronellal to menthol. *Appl. Catal. A: Gen.* **2007**, *317*, 171−174.

(9) Milone, C.; Gangemi, C.; Neri, G.; Pistone, A.; Galvagno, S. Selective one step synthesis of (−)-menthol from (+)-citronellal on Ru supported on modified SiO_2. *Appl. Catal. A: Gen.* **2000**, *199*, 239−244.

(10) Adilina, I. B.; Pertiwi, R.; Sulaswatty, A. Conversion of (±) -citronellal and its derivatives to (−) -menthol using bifunctional. *Biopropal Industri* **2015**, *6*, 1−6.

(11) Nie, Y.; Chuah, G. K.; Jaenicke, S. Domino-cyclisation and hydrogenation of citronellal to menthol over bifunctional Ni/Zr-Beta and Zr-beta/Ni-MCM-41 catalysts. *Chem. Commun.* **2006**, 790−792.

(12) Cortés, C. B.; Galván, V. T.; Pedro, S. S.; García, T. V. One pot synthesis of menthol from (±)-citronellal on nickel sulfated zirconia catalysts. *Catal. Today* **2011**, *172*, 21−26.

(13) Iftitah, E. D.; Muchalal, M.; Trisunaryanti, W.; Armunanto, R.; Psaro, R.; Ravasio, N.; Santoro, F.; Sordelli, L. One pot transformation of citronellal to menthol over Ni/γ-Al_2O_3. *J. Appl. Sci. Res.* **2011**, *7*, 680−689.

(14) Trasarti, A. F.; Marchi, A. J.; Apesteguía, C. R. Design of catalyst systems for the one-pot synthesis of menthols from citral. *J. Catal.* **2007**, *247* (2), 155−165.

(15) Nie, Y.; Jaenicke, S.; Chuah, G. K. Zr-zeolite beta: A new heterogeneous catalyst system for the highly selective cascade transformation of citral to (±)-menthol. *Chem.—Eur. J.* **2009**, *15* (8), 1991−1999.

(16) Mäki-Arvela, P.; Kumar, N.; Kubička, D.; Nasir, A.; Heikkilä, T.; Lehto, V. P.; Sjöholm, R.; Salmi, T.; Murzin, D. Y. One-pot citral transformation to menthol over bifunctional micro-and mesoporous metal modified catalysts: Effect of catalyst support and metal. *J. Mol. Catal. A: Chem.* **2005**, *240* (1−2), 72−81.

(17) Vajglová, Z.; Navas, M.; Mäki-Arvela, P.; Eränen, K.; Kumar, N.; Peurla, M.; Murzin, D. Y. Transformations of citral over bifunctional Ru-HY-80 extrudates in a continuous reactor. *Chem. Eng. J.* **2022**, *429*, 132190.

(18) Vajglová, Z.; Mäki-Arvela, P.; Eränen, K.; Kumar, N.; Peurla, M.; Murzin, D. Y. Catalytic transformations of citral in a continuous flow over bifunctional Ru-MCM-41 extrudates. *Catal. Sci. Techn.* **2021**, *11* (8), 2873−2884.

(19) Negoi, A.; Teinz, K.; Kemnitz, E.; Wuttke, S.; Parvulescu, V. L.; Coman, S. M. Bifunctional nanoscopic catalysts for the one-pot synthesis of (±)-menthol from citral. *Top. Catal.* **2012**, *55* (7), 680−687.

(20) Simakova, I.; Mäki-Arvela, P.; Martínez-Klimov, M.; Muller, J.; Vajglová, Z.; Peurla, M.; Eränen, K.; Murzin, D. Yu. Continuous synthesis of menthol from citronellal and citral over Ni-Beta-zeolite-sepiolite composite catalyst. *Appl. Catal. A: Gen.* **2022**, *636*, 118586.

(21) Simakova, I. L.; Vajglová, Z.; Mäki-Arvela, P.; Eränen, K.; Hupa, L.; Peurla, M.; Mäkilä, E. M.; Wärnå, J.; Murzin, D. Yu. Citral-to-menthol transformations in a continuous reactor over Ni/mesoporous aluminosilicate extrudates containing a sepiolite clay binder. *Org. Proc. Res.* **2022**, *26*, 387−403.

(22) Nefzi, H.; Abderrabba, M.; Ayadi, S.; Labidi, J. Formation of palygorskite clay from treated diatomite and its application for the removal of heavy metals from aqueous solution. *Water* **2018**, *10* (9), 1257.

(23) Xie, A.; Zhou, X.; Huang, X.; Ji, L.; Zhou, W.; Luo, S.; Yao, C. Cerium-loaded MnOx/attapulgite catalyst for the low-temperature NH_3-selective catalytic reduction. *J. Ind. Eng. Chem.* **2017**, *49*, 230−241.

(24) Guo, S.; Shi, L. Synthesis of succinic anhydride from maleic anhydride on Ni/diatomite catalysts. *Catal. Today* **2013**, *212*, 137−141.

(25) Anderson, J. A.; Rodrigo, M. T.; Daza, L.; Mendioroz, S. Influence of the support in the selectivity of nickel/clay catalysts for vegetable oil hydrogenation. *Langmuir* **1993**, *9* (10), 2485−2490.

(26) Zecevic, J.; Vanbutsele, G.; de Jong, K. P.; Martens, J. A. Nanoscale intimacy in bifunctional catalysts for selective conversion of hydrocarbons. *Nature* **2015**, *528* (7581), 245−248.

(27) Harmel, J.; Roberts, T.; Zhang, Z.; Sunley, G.; de Jongh, P.; de Jong, K. P. Bifunctional molybdenum oxide/acid catalysts for hydroisomerization of n-heptane. *J. Catal.* **2020**, *390*, 161−169.

(28) Vajglová, Z.; Kumar, N.; Peurla, M.; Hupa, L.; Semikin, K.; Sladkovskiy, D. A.; Murzin, D. Yu. Effect of the preparation of Pt-modified zeolite beta-bentonite extrudates on their catalytic behavior in n-hexane hydroisomerization. *Ind. Eng. Chem. Res.* **2019**, *58* (25), 10875−10885.

(29) Vajglová, Z.; Simakova, I. L.; Eränen, K.; Mäki-Arvela, P.; Kumar, N.; Peurla, M.; Tolvanen, S.; Efimov, A.; Hupa, L.; Peltonen, J.; Murzin, D. Yu. The physicochemical and catalytic properties of clay extrudates in cyclization of citronellal. *Appl. Catal. A: Gen.* **2022**, *629*, 118426.

(30) Emeis, C. A. Determination of integrated molar extinction coefficients for infrared absorption bands of pyridine adsorbed on solid acid catalysts. *J. Catal.* **1993**, *141*, 347−354.

(31) *Powder Diffraction File database PDF-2*; International Centre for Diffraction Data: USA, 2009.

(32) Vajglova, Z.; Kumar, N.; Mäki-Arvela, P.; Eränen, K.; Peurla, M.; Hupa, L.; Nurmi, M.; Toivakka, M.; Murzin, D. Y. Synthesis and physicochemical characterization of shaped catalysts of β and Y

zeolites for cyclization of citronellal. *Ind. Eng. Chem. Res.* **2019**, *58* (39), 18084−18096.
(33) Boudriche, L.; Chamayou, A.; Calvet, R.; Hamdi, B.; Balard, H. Influence of different dry milling processes on the properties of an attapulgite clay, contribution of inverse gas chromatography. *Powder technology* **2014**, *254*, 352−363.
(34) Nugraha, R. E.; Prasetyoko, D.; Bahruji, H.; Suprapto, S.; Asikin-Mijan, N.; Oetami, T. P.; Dai-Veit, N. Vo.; Taufiq-Yap, Y. H. Lewis acid Ni/Al-MCM-41 catalysts for H_2-free deoxygenation of Reutealis trisperma oil to biofuels. *RSC Adv.* **2021**, *11* (36), 21885−21896.
(35) Yang, L.; Huang, J.; Cen, J.; Chen, D. L.; Zeng, H.; Rui, Z.; Luque, R.; Duan, P. Lewis acid (Ni 2+, Co 2+/3+ or Zn 2+) modified electron-deficient Ir 4+ in IrO 2/CuO for promoting methane oxidation to ethanol and methanol. *J. Mater. Chem. A* **2021**, *9* (11), 7094−7101.
(36) Wei, Z.; Xia, T.; Ma, J.; Feng, W.; Dai, J.; Wang, Q.; Yan, P. Investigation of the lattice expansion for Ni nanoparticles. *Mater. Charact.* **2007**, *58* (10), 1019−1024.
(37) Quindimil, A.; De-La-Torre, U.; Pereda-Ayo, B.; Gonzalez-Marcos, J. A.; Gonzalez-Velasco, J. R. Ni catalysts with La as promoter supported over Y-and Beta-zeolites for CO2 methanation. *Appl. Catal. B: Env.* **2018**, *238*, 393−403.
(38) Wang, Y.; Liang, D.; Wang, C.; Chen, M.; Tang, Z.; Hu, J.; Yang, Z.; Zhang, H.; Wang, J.; Liu, S. Influence of calcination temperature of Ni/attapulgite on hydrogen production by steam reforming ethanol. *Renew. Energy* **2020**, *160*, 597−611.
(39) Bertero, N. M.; Trasarti, A. F.; Apesteguía, C. R.; Marchi, A. J. Liquid-phase dehydration of 1-phenylethanol on solid acids: Influence of catalyst acidity and pore structure. *Appl. Catal. A: Gen.* **2013**, *458*, 28−38.
(40) Chuah, G. K.; Liu, S. H.; Jaenicke, S.; Harrison, L. J. Cyclisation of citronellal to isopulegol catalysed by hydrous zirconia and other solid acids. *J. Catal.* **2001**, *200* (2), 352−359.

https://doi.org/10.1021/acs.iecr.2c02345
Ind. Eng. Chem. Res. 2022, 61, 12998−13010